A Closed-Form Approximated Expression for the Residual ISI Obtained by Blind Adaptive Equalizers with Gain Equal or Less than One

Simon KUPCHAN, Monika PINCHAS

Dept. of Electrical and Electronic Engineering, Ariel University of Samaria, Ariel 40700, Israel

simonkupchan@gmail.com, monika.pinchas@gmail.com

Abstract. *In this paper we propose for the real and two independent quadrature carrier cases, a closed-form approximated expression for the achievable residual Inter-Symbol Interference (ISI). The expression depends on the step-size parameter, equalizer's tap length, equalized output gain, input signal statistics, channel power and SNR. This expression is valid for blind adaptive equalizers where the error fed into the adaptive mechanism, which updates the equalizer's taps, can be expressed as a polynomial function of order three of the equalized output, and where the gain between the input and equalized output signal is less than, or equal to one, as in the case of Godard* $(gain = 1)$ *and WNEW* $(gain < 1)$ *algorithm. Since the channel power is measurable, or can be calculated if the channel coefficients are given, there is no need for simulation with various step-size parameters to reach the required residual ISI. In addition, we show two new equalization methods (gain dependent) which have improved equalization performance compared to Godard and WNEW.*

Keywords

ISI distortion, residual ISI, blind equalizer.

1. Introduction

The wireless bandwidth limitation by government regulations, the large number of wireless applications sharing the limited bandwidth and constantly increasing communication speeds accentuate the ISI distortion. This is the main limitation factor for increasing communication speed. Today, wireless networks, such as GSM transmit training sequences, take up to 16% [1] of the channel capacity. This can be eliminated by using blind equalizers to retrieve transmitted data through the noisy channels by eliminating training sequence transmission. Thus preserving channel capacity for the data communication, which will increase speed. To develop a new blind equalizer we need to evaluate its performance using the achievable residual ISI. Developing a new blind equalizer involves choosing the equalizer's tap length and step-size parameter for a particular application or channel. Formerly, we used time consuming simulation for performance assessment. This part of the development process can be eliminated by using the closed-form approximated expression for the achievable residual ISI developed by Pinchas [2] for the noiseless case and expanded for the noisy environment by the same author in [3]. Both of the above mentioned expressions [2], [3] work well for equalizers with equalized output gain equal to one, as in Godard [5]. In [4] the WNEW algorithm was developed showing excellent equalization performance while having the same computational burden as the Godard algorithm. But its equalized output gain is lower than one. Thus, the expressions for the residual ISI developed in [2] and [3] are not applicable for the WNEW [4] algorithm as shown in Section V.

In this work, we develop a new closed-form approximated expression for the residual ISI for blind adaptive equalizers with equalized output gain lower or equal to one. As a by-product we present two new equalization methods (gain dependent) with improved equalization performance compared to the WNEW [4] and Godard [5] algorithm.

The paper is organized as follows: After describing the system under consideration in Section 2, the closed-form approximated expression for the achievable residual lSI is introduced in Section 3. In Section 4 two new equalization methods are introduced. Simulation results for the new closed-form approximated expression for the residual ISI and the new developed algorithms (gain dependent) are given in Section 5. The conclusion is presented in Section 6.

2. System Description

The system under consideration is the same system as used in [2], [3] and recalled here in Fig. 1.

We use in the following the same assumptions done in [2], [3]:

1. The transmitted sequence $x[n]$ is a Quadrature Amplitude Modulated (QAM) constellation, where x_r and x_i

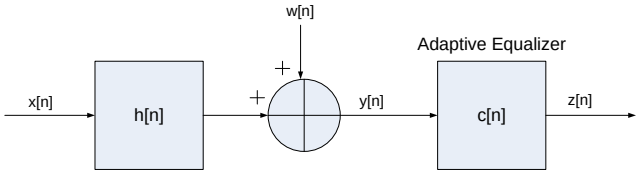

Fig. 1. Block diagram of the baseband communication system.

are the real and imaginary parts of $x[n]$ respectively and are independent. σ_x^2 is the variance of $x[n]$.

2. The unknown channel $h[n]$ is a possibly non-minimum phase linear time-invariant filter in which the transfer function has no "deep zeros", namely, the zeros lie sufficiently far from the unit circle.

3. The equalizer $c[n]$ is a tap-delay line.

4. The noise $w[n]$ is an additive Gaussian white noise with variance σ_w^2.

The sequence $x[n]$ is transmitted through the channel $h[n]$ and is corrupted with noise $w[n]$. Therefore, the equalizer's input sequence $y[n]$ may be written as:

$$y[n] = x[n] * h[n] + w[n] \tag{1}$$

where $*$ denotes the convolution operation. The equalized output signal is given by [2], [3]:

$$z[n] = y[n] * c[n] = x[n] * h[n] * c[n] + w[n] * c[n] \tag{2}$$

In the ideal case we have:

$$h[n] * c[n] = \alpha\delta[n-D]e^{j\theta} \tag{3}$$

where α is a constant gain between the input and equalized output signal, δ is the Kroneker delta function, D and θ are a constant delay and phase shift respectively. In the following, we denote $D = 0$ and $\theta = 0$ (as in [2], [3]). Thus, we write:

$$\tilde{s}[n] = h[n] * c_g[n] = \alpha\delta[n] + \xi[n] \tag{4}$$

where ξ stands for the difference (error) between the ideal value $c[n]$ and the guess $c_g[n]$ as stated in [3] and α is the equalizer's output gain. Substituting (4) into (2) yields:

$$z[n] = \alpha x[n] + p[n] + \beta\widetilde{w}[n] \tag{5}$$

where β is a noise gain factor, $p[n]$ is the convolutional noise, produced from the difference between the initial guess $c_g[n]$ and the ideal values for $c[n]$, $\beta\widetilde{w}[n] = w[n] * c_g[n]$ denotes the noise that passes through the equalizer.

The equalizer's update mechanism is defined by:

$$\underline{c}_{eq}[n+1] = \underline{c}_{eq}[n] - \mu \cdot \left(\frac{\partial F[n]}{\partial z[n]}\underline{y}^*[n]\right) \tag{6}$$

where μ is the equalizer's step size, $\underline{c}_{eq}[n]$ represents the current state of the equalizer's vector and $\underline{y}^*[n]$ is the input vector $y[n] = [y[n], \ldots, y[n-N+1]]^T$ where $()^*$ is the conjugate operator and N is the equalizer's tap length. In this paper the real part of $\frac{\partial F[n]}{\partial z[n]}$ is a polynomial function of order three of the equalized output defined (as in [2], [3]) by :

$$Re\left(\frac{\partial F[n]}{\partial z[n]}\right) = \left(a_1(z_r) + a_3(z_r)^3 + a_{12}(z_r)(z_i)^2\right) \tag{7}$$

where z_r , z_i are the real and imaginary parts of the equalized output $z[n]$ respectively and a_1, a_3, a_{12} are properties of the equalizer. The ISI is often used as a measure of performance in equalizer's applications, defined in [2]:

$$ISI = \frac{\sum_{\widetilde{m}} |\tilde{s}(\widetilde{m})|^2 - |\tilde{s}|^2_{\max}}{|\tilde{s}|^2_{\max}} \tag{8}$$

where $|s|_{max}$ is the component of $\tilde{s}$, given in (4), having the maximal absolute value.

In the next section we will develop a new closed-form approximated expression for the achievable residual lSI for blind adaptive equalizers where the gain of the equalized output is less than or equal to one.

2.1 ISI Performance

In this section we develop a closed-form approximated expression for the expected residual ISI as a function of the constellation input statistics, equalizer's tap length, equalized output gain, step-size parameter, channel power and SNR.

Theorem. For the following assumptions:

1. The convolutional noise p[n], is a zero mean, white Gaussian process with variance $\sigma_p^2 = E[p[n]p^*[n]]$, where $E[\,]$ stands for the expectation operator.

2. The variance and higher moments of the source signal $x[n]$ are known.

3. The convolutional noise p[n] and the source signal are independent.

4. α is the gain between the input and equalized output signal.

5. β is the noise gain factor for input noise.

6. $\max(|\tilde{s}|^2) = \alpha^2$.

7. $\frac{\partial F[n]}{\partial z[n]}$ can be expressed as a polynomial function of order three of the equalized output namely as $P(z)$.

The residual ISI expressed in dB units is defined as:

$$ISI = 10\log_{10}(m_p) - 10\log_{10}(\alpha^2) - 10\log_{10}(\sigma_{x_r}^2) \tag{9}$$

where:

$$m_p = \min[Sol_1^{mp_1}, Sol_2^{mp_1}] \text{ for } Sol_1^{mp_1} > 0 \text{ and } Sol_2^{mp_1} > 0$$

or

$$m_p = \max[Sol_1^{mp_1}, Sol_2^{mp_1}] \text{ for } Sol_1^{mp_1} \cdot Sol_2^{mp_1} < 0.$$

$Sol_1^{mp_1}$ and $Sol_2^{mp_1}$ are defined by:

$$Sol_1^{mp_1} = \frac{-B_1 + \sqrt{B_1^2 - 4A_1C_1B}}{2A_1},$$
$$Sol_2^{mp_1} = \frac{-B_1 - \sqrt{B_1^2 - 4A_1C_1B}}{2A_1},$$

$$\begin{aligned} A_1 =& B\left(45\alpha^2 m_2 a_3^2 + 18\alpha^2 m_2 a_3 a_{12} + 9\alpha^2 m_2 a_{12}^2 + \right. \\ & \left. 6a_1 a_3 + 2a_1 a_{12}\right) - 2\left(3a_3 + a_{12}\right) + \\ & B\left(45a_3^2 + 18a_3 a_{12} + 9a_{12}^2\right)\beta^2\sigma_{\widetilde{w}_r}^2, \end{aligned}$$

$$\begin{aligned} B_1 =& \left(B\left(12\alpha^4 m_2^2 a_3 a_{12} + 6\alpha^4 m_2^2 a_{12}^2 + 12\alpha^2 m_2 a_1 a_3 + \right.\right. \\ & 4\alpha^2 m_2 a_1 a_{12} + a_1^2 + 15\alpha^4 m_4 a_3^2 + 2\alpha^4 m_4 a_3 a_{12} + \\ & \left.\left.\alpha^4 m_4 a_{12}^2\right) - 2\left(a_1 + 3\alpha^2 m_2 a_3 + \alpha^2 m_2 a_{12}\right)\right) + \\ & B\left(45a_3^2 + 18a_3 a_{12} + 9a_{12}^2\right)\beta^4\sigma_{\widetilde{w}_r}^4 + \\ & \left(B\left(90\alpha^2 m_2 a_3^2 + 36\alpha^2 m_2 a_3 a_{12} + 12a_1 a_3 + \right.\right. \\ & \left.\left.18\alpha^2 m_2 a_{12}^2 + 4a_1 a_{12}\right) - 2a_{12} - 6a_3\right)\beta^2\sigma_{\widetilde{w}_r}^2, \end{aligned}$$

$$\begin{aligned} C_1 =& \left(2\alpha^4 m_2^2 a_1 a_{12} + \alpha^2 m_2 a_1^2 + 2\alpha^6 m_4 m_2 a_3 a_{12} + \right. \\ & \left.\alpha^6 m_4 m_2 a_{12}^2 + 2\alpha^4 m_4 a_1 a_3 + \alpha^6 m_6 a_3^2\right) + \\ & \left(15a_3^2 + 6a_3 a_{12} + 3a_{12}^2\right)\beta^6\sigma_{\widetilde{w}_r}^6 + \\ & \left(45\alpha^2 m_2 a_3^2 + 18\alpha^2 m_2 a_3 a_{12} + 9\alpha^2 m_2 a_{12}^2 + 6a_1 a_3 + \right. \\ & \left. 2a_1 a_{12}\right)\beta^4\sigma_{\widetilde{w}_r}^4 + \\ & \left(a_1^2 + 12\alpha^2 m_2 a_1 a_3 + 4\alpha^2 m_2 a_1 a_{12} + 15\alpha^4 m_4 a_3^2 + \right. \\ & 12\alpha^4 m_2^2 a_3 a_{12} + 2\alpha^4 m_4 a_3 a_{12} + \\ & \left.\alpha^4 m_4 a_{12}^2 + 6\alpha^4 m_2^2 a_{12}^2\right)\beta^2\sigma_{\widetilde{w}_r}^2, \end{aligned} \tag{10}$$

$$B = \mu N \sigma_x^2 \left(\sum_{k=0}^{k=R-1} |h_k[n]|^2 + \frac{1}{SNR}\right) \tag{11}$$

where $m_\chi = E[x_r^\chi]$, $\sigma_{\widetilde{w}_r}^2 = \frac{\sigma_{x_r}^2}{SNR\sum_{k=0}^{k=R-1}|h_k[n]|^2}$, R is the channel's length, $SNR = \sigma_x^2/\sigma_w^2$ and a_1, a_3, a_{12} are the properties of the chosen equalizer and found via (7).

Proof. We begin our proof by recalling from [2] the expression for $E[\triangle(p_r^2)]$ (where p_r is the real part of $p[n]$ and $\triangle(p_r^2) = p_r^2[n+1] - p_r^2[n]$:

$$\begin{aligned} & E[\triangle(p_r^2)] = \\ & -2E\left[p_r\left(\mu P_r(z)\sum_{m=0}^{m=l} y[n-m]y^*[n-m]\right)\right] + \\ & E\left[\left(-\mu P_r(z)\sum_{m=0}^{m=l} y[n-m]y^*[n-m]\right)^2\right] \end{aligned} \tag{12}$$

where $P_r(z)$ is the real part of $P(z)$ and is given according to [2] as:

$$P_r(z) = \left(a_1(z_r) + a_3(z_r)^3 + a_{12}(z_r)(z_i)^2\right) \tag{13}$$

where z_r and z_i are the real and imaginary parts of (5) and equal to:

$$\begin{aligned} z_r &= \alpha x_r + p_r + \beta\widetilde{w}_r \\ z_i &= \alpha x_i + p_i + \beta\widetilde{w}_i \end{aligned} \tag{14}$$

where α and β may not be equal. In this paper, $p_r = p_r[n]$ where p_r and p_i are the real and imaginary parts of $p[n]$ respectively. Next, we calculate (12) in the same way as in [3]. We substitute (14) into (13) and evaluate (12) by using (14) and (13). Thus, we obtain for the latter stages of the convergence state:

$$E\left[\triangle\left(p_r^2\right)\right] \cong BA_1 m_p^2 + BB_1 m_p + B^2 C_1 \tag{15}$$

where $E[p_r[n]^2] = m_p$ and B, B_1, A_1, C_1 are given in (10). Note that B, B_1, A_1, C_1 are different from those obtained in [3] due to the α and β parameters. In the latter stages of the deconvolution process, we may write: $E\left[\triangle\left(p_r^2\right)\right] \cong 0$. Thus, setting (15) to zero and solving the equation for m_p will lead to the solution for m_p given in (10).

Now to obtain the expression for the ISI given in (9) we use (2) and (5) thus we write for the noiseless case:

$$\begin{aligned} & E[z[n]z[n]^*] = \\ & E[(\widetilde{s}[n] * x[n])(\widetilde{s}[n] * x[n])^*] = \\ & E[x[n]x[n]^*]\sum_{\widetilde{m}}|\widetilde{s}[\widetilde{m}]|^2 = \sigma_x^2\sum_{\widetilde{m}}|\widetilde{s}[\widetilde{m}]|^2, \end{aligned} \tag{16}$$

$$\begin{aligned} & E[z[n]z[n]^*] = \\ & E\left[(\alpha x[n] + p[n] + \beta w[n])(\alpha x[n] + p[n] + \beta w[n])^*\right] = \\ & \alpha^2 E[x[n]x[n]^*] + E[p[n]p[n]^*] = \alpha^2\sigma_x^2 + \sigma_p^2. \end{aligned} \tag{17}$$

By comparing (16) with (17) we obtain:

$$\sigma_p^2 = \sigma_x^2\left[\sum_{\widetilde{m}}|\widetilde{s}[\widetilde{m}]|^2 - \alpha^2\right]. \tag{18}$$

Dividing (18) by a^2 leads to:

$$\frac{\sigma_p^2}{\alpha^2} = \sigma_x^2\frac{\left[\sum_{\widetilde{m}}|\widetilde{s}(\widetilde{m})|^2 - \alpha^2\right]}{\alpha^2}, \quad |\widetilde{s}|_{max}^2 = \alpha^2 \tag{19}$$

which with the help of (8) can be written as:

$$ISI = \frac{\sigma_p^2}{\alpha^2 \sigma_x^2}. \tag{20}$$

Since $\sigma_p^2/\sigma_x^2 = \sigma_{p_r}^2/\sigma_{x_r}^2$ and the ISI is measured in the logarithmic scale we have (9).

Next, we turn to the various steps that lead to the expression for $\sigma_{\widetilde{w}_r}^2$:

$$\beta\widetilde{w}[n] = c_g[n] * w[n] \tag{21}$$

which with the help of (4) can be written as:

$$\begin{aligned} &\beta\widetilde{w}[n] * h[n] = c_g[n] * w[n] * h[n] = \\ &w[n] * \tilde{s}[n] = w[n] * (\alpha\delta[n] + \xi[n]) \end{aligned} \tag{22}$$

thus for $\xi[n] \to 0$ (for the ideal case) we have:

$$\beta^2 \sigma_{\widetilde{w}_r}^2 \cong \alpha^2 \sigma_{w_r}^2 \frac{1}{\sum_{k=0}^{R-1} |h_k[n]|^2} \tag{23}$$

where $\sigma_{\widetilde{w}_r}^2$ and $\sigma_{w_r}^2$ are the variances of the real part of $\widetilde{w}[n]$ and $w[n]$ respectively. From (23) we may see that for $\xi[n] \to 0$ and $\alpha = \beta$ we return to the expression for $\sigma_{\widetilde{w}_r}^2$ used in (10). This is the same expression for $\sigma_{\widetilde{w}_r}^2$ used in [3] for the case where the equalized output gain is equal to one.

This completes our *Proof*.

2.2 The ANEW Equalizer

In this section we develop a new equalization method, namely we propose a new function for $Re\{\frac{\partial F[n]}{\partial z[n]}\}$. As already mentioned earlier in this paper, we write $E\left[\triangle\left(p_r^2\right)\right] \cong 0$ for the latter stages of the deconvolutional process. Therefore, by setting (15) to zero and dividing (15) by B (for $B \neq 0$), we may see that the convolutional noise power m_p does not converge in the steady state approximately to zero unless $C_1 = 0$ as stated in [3]. C_1 (10) depends on the constellation input statistics and on the algorithm itself via a_1, a_3 and a_{12}. By minimizing $C1$ with respect to the algorithm parameters (a_1, a_3, a_{12}) we may obtain a new equalizer.

Theorem. For the following assumptions:

1. The transmitted sequence $x[n]$ belongs to the square QAM constellation, thus a_{12} is set to zero.
2. No noise is added $\sigma_{\widetilde{w}_r}^2 = 0$

The real part of $\frac{\partial F[n]}{\partial z[n]}$ can be written as:

$$Re\left(\frac{\partial F[n]}{\partial z[n]}\right) = \left(a_1(z_r) + a_3(z_r)^3\right) \tag{24}$$

with

$$a_1 = -\alpha; \quad a_3 = \frac{m_2}{\alpha m_4}; \quad a_{12} = 0. \tag{25}$$

Proof. We start the proof from recalling C_1 (10) and deleting there a_{12} and the noise component. Thus having:

$$C_1 = \alpha^2 m_2 a_1^2 + 2\alpha^4 m_4 a_1 a_3 + \alpha^6 m_6 a_3^2. \tag{26}$$

Now, minimizing (26) with respect to the coefficients a_1, a_3, α and then setting the relevant equations to zero, we obtain:

$$\frac{\partial C_1}{\partial \alpha} = 2\alpha m_2 a_1^2 + 8\alpha^3 m_4 a_1 a_3 + 6\alpha^5 m_6 a_3^2 = 0, \tag{27}$$

$$\frac{\partial C_1}{\partial a_1} = 2\alpha^2 m_2 a_1 + 2\alpha^4 m_4 a_3 = 0, \tag{28}$$

$$\frac{\partial C_1}{\partial a_3} = 2\alpha^4 m_4 a_1 + 2\alpha^6 m_6 a_3 = 0. \tag{29}$$

By solving (27), (28) and (29) the trivial solution ($a_1 = 0$, $a_3 = 0$) is obtained, which indicates that no equalizer exists. To find a non-trivial solution we set a_1 to $(-\alpha)$, which leads to two different solutions for a_3. The first solution is given in (25) obtained via (28) while the second solution obtained via (29) is given by:

$$a_1 = -\alpha; \quad a_3 = \frac{m_4}{\alpha m_6}; \quad a_{12} = 0. \tag{30}$$

Now, we turn to compare the two solutions (25) and (30), by substituting each of them into (26) and evaluate (26) for the 16QAM input case. For the 16QAM input case we have: $m_2 = 5$, $m_4 = 41$ and $m_6 = 365$. Thus we have:

$$C_1 \cong 0.43\alpha^4, \quad \text{for Case A}, \tag{31}$$

$$C_1 \cong 0.39\alpha^4, \quad \text{for Case B} \tag{32}$$

where Case A and Case B were obtained by substituting (25) and (30) into (26) respectively. According to (31) and (32), Case B may lead to a lower residual ISI in the steady state compared to Case A. However, the difference between the two cases (A, B) as appears in (31) and (32) is so small, that we may not see any difference in the equalization performance from the residual ISI point of view. In addition, we observe according to (31) and (32) that a smaller value for α may lead to a lower residual ISI. Note that for $\alpha = 0$ we obtain $C_1 = 0$ (perfect equalization), but for this case no equalizer exists (refer to (5)), thus no perfect equalization is obtained for $\alpha = 0$.
This completes our *Proof*.

2.3 Simulation

In this section we compare the usefulness of our new proposed expression for the residual ISI (9) with the expression for the residual ISI obtained in [3]. In the following we use (25) and (30) to define two new equalization methods, which we denote as ANEW and BNEW respectively. We compare the equalization performance obtained from the ANEW (with various values for α) and BNEW algorithm with Godard [5] and WNEW [4]. The equalizers were initialized by setting the center tap to one and all other taps to

zero. The equalizer's taps according to Godard were updated by:

$$\begin{aligned} \underline{c}_G[n+1] &= \underline{c}_G[n] - \mu_G G \underline{y}^*[n], \\ G &= \left(|z|^2 - \frac{E[|x|^4]}{E[|x|^2]} \right) z \end{aligned} \tag{33}$$

where $z = z[n]$, $x = x[n]$, $E[\,]$ is the expectation operator, $|\,|$ is the absolute operator, μ_G is the step-size parameter and a_1, a_3 and a_{12} were defined as a_1^G, a_3^G and a_{12}^G respectively and given by:

$$a_1^G = -\frac{E[|x|^4]}{E[|x|^2]}, \quad a_3^G = 1, \quad a_{12}^G = 1. \tag{34}$$

The equalizer's taps for WNEW [4] algorithm were updated according to:

$$\begin{aligned} \underline{c}_W[n+1] &= \underline{c}_W[n] - \mu_W W_{new} \underline{y}^*[n], \\ W_{new} &= \frac{1}{m_2} \left(z_r^3 + j z_i^3 \right) - z \end{aligned} \tag{35}$$

where μ_W is the step-size parameter and a_1, a_3 and a_{12} were defined as a_1^W, a_3^W and a_{12}^W respectively and given by:

$$a_1^W = -1, \quad a_3^W = -\frac{1}{m_2}, \quad a_{12}^W = 0. \tag{36}$$

The equalizer's taps for ANEW algorithm were updated according to:

$$\begin{aligned} \underline{c}_A[n+1] &= \underline{c}_A[n] - \mu_A A_{new} \underline{y}^*[n], \\ A_{new} &= \frac{m_2}{\alpha m_4} \left(z_r^3 + j z_i^3 \right) - \alpha z \end{aligned} \tag{37}$$

where μ_A is the step-size parameter and a_1, a_3 and a_{12} were substituted from (25). The equalizer taps for BNEW algorithm were updated according to:

$$\begin{aligned} \underline{c}_B[n+1] &= \underline{c}_B[n] - \mu_B B_{new} \underline{y}^*[n], \\ B_{new} &= \frac{m_4}{\alpha m_6} \left(z_r^3 + j z_i^3 \right) - \alpha z \end{aligned} \tag{38}$$

where μ_B is the step-size parameter and a_1, a_3 and a_{12} were substituted from (30). Two input sources were used: the 16QAM and 64QAM modulations with $\pm\{1,3\}$ and $\pm\{1,3,5,7\}$ levels respectively, for in-phase and quadrature components. Four different channels were considered.

Channel1 (initial lSI = 0.44): The channel parameters were determined according to Shalvi and Weinstein [10]:
h_n = (0 for $n < 0$; -0.4 for $n = 0$; $0.84 \cdot 0.4^{n-1}$ for $n > 0$).

Channel 2 (initial lSI = 0.5): The channel parameters were determined according to Fiori [11]:
h_n = (-0.0144, 0.0006, 0.0427, 0.0090, -0.4842, -0.0376, 0.8163, 0.0247, 0.2976, 0.0122, 0.0764, 0.0111, 0.0162, 0.0063).

Channel 3 (initial lSI = 0.88): The channel parameters were determined according to Pinchas [2]:
h_n = (0.4851, -0.72765, -0.4851)

Channel4 (initial lSI = 0.44): The channel parameters were determined according to Shalvi and Weinstein [10]:
h_n = (0 for $n < 0$; -0.4 for $n = 0$; $0.84 \cdot 0.4^{n-1}$ for $n > 0$) and normalized to $hh^T = 0.507$.

Let us start with the comparison of our closed-form approximated expression for the residual ISI (9) with the one obtained in [3]. Note the main difference between the two expressions (9) and [3], is in the α and β parameters. In [3] $\alpha = \beta = 1$, while in our case α and β receive various values.

Fig. 2 and Fig. 3 show the equalization performance comparison from the residual ISI point of view obtained by (9), [3] with the simulated results obtained by the WNEW algorithm, for the 16QAM input case and SNR values of 10 dB and 30 dB respectively. According to Fig. 2 and Fig. 3 the residual ISI obtained by (9) is very close to the simulated results, while this is not the case with the residual ISI obtained by [3].

Fig. 4 to Fig. 7 show the simulated performance of the WNEW equalization method for the 16QAM and 64QAM input case, namely the ISI as a function of iteration number for various step-size parameters, channel characteristics, equalizer's tap length and various SNR values, compared with the calculated residual ISI expression (9) used with $\alpha = 0.84$ and $\beta = 0.58$. Figs. 4 – 7 show a high correlation between the simulated results and those calculated with (9).

Fig. 8 and Fig. 9 show the simulated performance of the ANEW equalization method with $\alpha = 0.8$ for the 16QAM and 64QAM input case, namely the ISI as a function of iteration number for various step-size parameters, Channel characteristics and various SNR values, compared with the calculated residual ISI expression (9) used with $\alpha = 0.8$ and $\beta = 0.73$. Fig. 8 and Fig. 9, point to a high correlation between the simulated results and those calculated with (9).

Fig. 10 to Fig. 13 show the simulated performance of the ANEW equalization method with $\alpha = 1$ for the 16QAM and 64QAM input case, namely the ISI as a function of iteration number for various step-size parameters, channel characteristics, equalizer's tap length and various SNR values, compared with the calculated residual ISI expression (9) used with $\alpha = 1$ and $\beta = 0.93$. Fig. 10 to Fig. 13 indicate a high correlation between the simulated and calculated performance (9) of the achievable residual lSI.

Fig. 14 to Fig. 16 show the simulated performance of Godard's equalization method for the 16QAM and 64QAM input case, namely the ISI as a function of iteration number for various step-size parameters, channel characteristics, equalizer's tap length and various SNR values, compared with the calculated residual ISI expression (9) used with $\alpha = 1$ and $\beta = 1$. Fig. 14 to Fig. 16 show a high correlation between the simulated results and those calculated with (9).

Next, we turn to compare equalization performance obtained from the ANEW and BNEW algorithm. Fig. 17 and Fig. 18 show the ISI comparison between the simulated performance of the two equalization methods ANEW and

BNEW with $\alpha = 1$ (for both methods). The comparison was carried out for the 16QAM and 64QAM input case, for various step-size parameters, channel characteristics and SNR values of 10 dB and 30 dB. According to Fig. 17 and Fig. 18, ANEW and BNEW have approximately the same equalization performance.

Now, we turn to regarding the equalization performance comparison between ANEW with various gains ($\alpha = 0.8$, $\alpha = 1$), WNEW [4] and Godard [5].

Fig. 19 and Fig. 20 show the equalization performance comparison between the simulated performance obtained by the ANEW algorithm with two different values for α ($\alpha = 0.8$ and $\alpha = 1$), namely the ISI as a function of iteration number for Channel 1, 16QAM input case and SNR values of 10 dB and 30 dB. According to Fig. 19 and Fig. 20 and backed up by (31), a lower gain (α) leads to a lower residual ISI, hence to a better residual ISI performance.

Fig. 21 and Fig. 22 show the equalization performance comparison between the simulated performance obtained by the ANEW and WNEW equalization algorithm, namely the ISI as a function of iteration number for Channel 1, 16QAM input case and SNR values of 10 dB and 30 dB. According to Fig. 21 and Fig. 22 almost no difference is seen between the ANEW and WNEW equalizer. Note, that the ANEW equalizer was simulated with $\alpha = 1$. A lower value for α might have led the ANEW algorithm to a lower residual ISI compared to the WNEW method (please refer to Fig. 19 and Fig. 20).

Fig. 23 to Fig. 28 show the equalization performance comparison between the simulated performance obtained by the ANEW and Godard's equalization algorithm, namely the ISI as a function of iteration number for various channels, 16QAM and 64QAM input case, various step-size parameters, equalizer's tap length and SNR values of 10 dB and 30 dB. As seen from Fig. 23 to Fig. 28 the ANEW equalizer has improved equalization performance compared to Godard [5]. The improved equalization performance is seen in the residual ISI as well as in the convergence speed.

2.4 Conclusion

In this work, we have developed a new closed-form approximated expression for the achievable residual ISI valid for blind adaptive equalizers, where the gain between the input and equalized output signal is less than or equal to one, as is in the case of Godard [5], WNEW [4] and ANEW algorithm. Thus, the expressions for the residual ISI obtained in previous papers ([2], [3]) are special cases of our new proposed expression. In addition, we have developed two new equalization (α dependant) algorithms. The new algorithms were called ANEW and BNEW, shown to have improved equalization performance compared to Godard and WNEW. The new algorithms (ANEW and BNEW) have the same computational complexity as the classical Godard and WNEW algorithm.

Acknowledgements

We would like to thank the anonymous reviewers for their helpful comments.

References

[1] *Digital Cellular Telecommunications System (Phase 2+); Multiplexing and Multiple Access on the Radio Path*. ETSI European Telecommunications Standards Institute, ICS: 33.060.50, 1996.

[2] PINCHAS, M. A closed approximated formed expression for the achievable residual intersymbol interference obtained by blind equalizers. *Signal Processing (Eurasip)*, 2010, vol. 90, no. 6, p. 1940 - 1962.

[3] PINCHAS, M. A new closed approximated formed expression for the achievable residual intersymbol interference obtained by blind equalizers for the noisy case. In *IEEE International Conference on Wireless Communications, Networking and Information Security (WCNIS*. Beijing, (China), 2010, p. 26 - 30.

[4] PINCHAS, M., BOBROVSKY, B. Z. A maximum entropy approach for blind deconvolution. *Signal Processing (Eurasip)*, 2006, vol. 86, no. 10, p. 2913 - 2931.

[5] GODARD, D. Self-recovering equalization and carrier tracking in two- dimenional data communication system. *IEEE Transactions on Communications*, 1980, vol. 28, no. 11, p. 1867 - 1875.

[6] PINCHAS, M. A MSE optimized polynomial equalizer for 16QAM and 64QAM constellation. *Signal, Image and Video Processing*, 2011, vol. 5, no. 1, p. 29 - 37.

[7] PINCHAS, M. A novel expression for the achievable MSE performance obtained by blind adaptive equalizers. *Signal, Image and Video Processing*, 2013, vol. 7, no. 1, p. 67 - 74.

[8] GI-HONG IM, CHEOL-JIN PARK, HUI-CHUL WON A blind equalization with the sign algorithm for broadband access. *IEEE Communications Letters*, 2001, vol. 5, no. 2, p. 70 - 72.

[9] LAZARO, M., SANTAMARIA, I., ERDOGMUS, D., HILD, K. E., PANTALEON, C., PRINCIPE, J. C. Stochastic blind equalization based on PDF fitting using Parzen estimator. *IEEE Transactions on Signal Processing*, 2005, vol. 53, no. 2, p. 696 - 704.

[10] SHALVI O., WEINSTEIN, E. New criteria for blind deconvolution of nonminimum phase systems (channels). *IEEE Transactions on Information Theory*, 1990, vol. 36, no. 2, p. 312 - 321.

[11] SHALVI, O., WEINSTEIN, E. Super-exponential methods for blind deconvolution. *IEEE Transactions on Information Theory*, 1993, vol. 39, no. 2, p. 504 - 519.

[12] NIKIAS, C., PETROPULU A. P. (Eds.) *Higher-Order Spectra Analysis: A Non-linear Signal Processing Framework.* Prentice-Hall, 1993, p. 419 - 425.

About Authors ...

Monika PINCHAS is with the Ariel University. She is the Head of the graduate program at the faculty of Electrical and Electronic Engineering. Her research interests are in the area of blind equalization, frequency synchronization in OFDM systems and network synchronization where she has published several papers in leading journals and published two books. She was the CTO at Resolute Networks, man-

aged the hardware group at Radiotel wireless transmission line of products, leading the development of modem technology. She worked at Tadiran Communication where she was recognized as an expert and worked for Scitex in the design and implementation of hardware systems.

Simon KUPCHAN received the B.Tech. degree in Electrical Engineering from Ariel University Center, Ariel, Israel, in 2006. From 2004, he worked in Infra-Com Ltd., Netanya, Israel, where he was HW digital designer in the R&D team. Since 2010, he has been with Orsan Medical Technologies Ltd. Netanya, Israel, where he is currently senior HW digital designer in the R&D team.

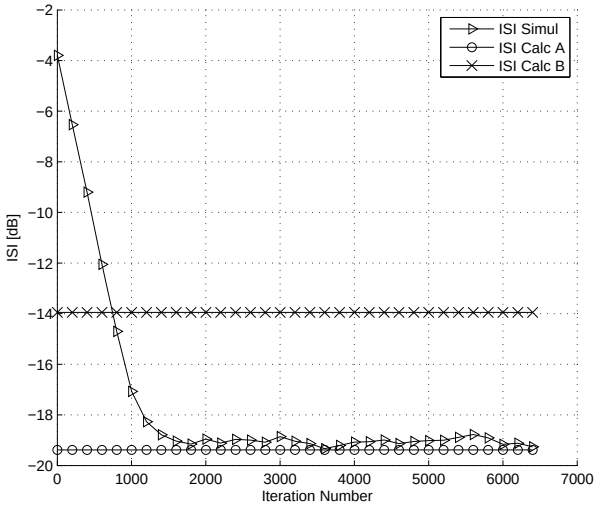

Fig. 2. A comparison between the simulated (with WNEW algorithm) and calculated residual ISI according to (9) (ISI Calc A) and [3] (ISI Calc B) for the 16QAM source going through Channel 1 and SNR of 10 dB. The averaged results were obtained in 100 Monte Carlo trials. The equalizer's tap length and step-size parameter were set to 13 and 0.0004 respectively. α and β gain parameters were set to 0.84 and 0.58 respectively.

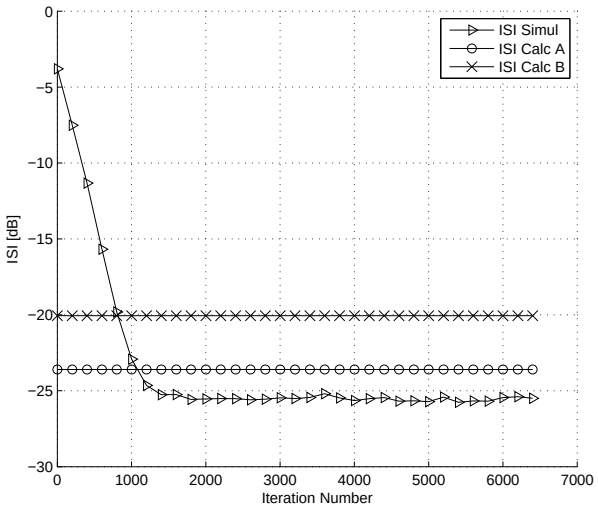

Fig. 3. A comparison between the simulated (with WNEW algorithm) and calculated residual ISI according to (9) (ISI Calc A) and [3] (ISI Calc B) for the 16QAM source going through Channel 1 and SNR of 30 dB. The averaged results were obtained in 100 Monte Carlo trials. The equalizer's tap length and step-size parameter were set to 13 and 0.0004 respectively. α and β gain parameters were set to 0.84 and 0.58 respectively.

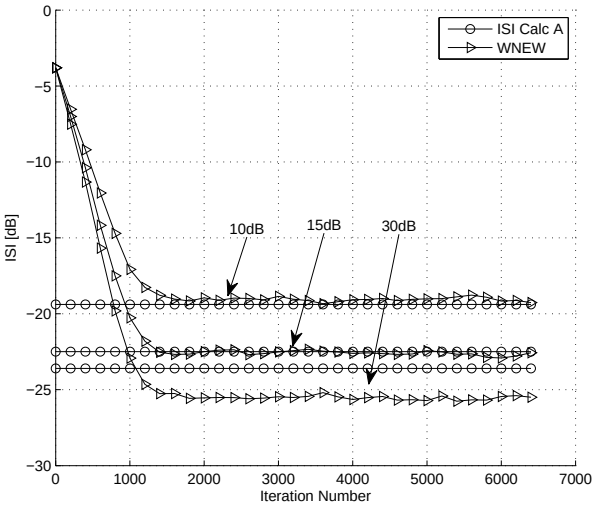

Fig. 4. A comparison between the simulated (with WNEW algorithm) and calculated residual ISI (9) (ISI Calc A) for the 16QAM source going through Channel 1 with various SNR values. The averaged results were obtained in 100 Monte Carlo trials. The equalizer's tap length and step-size parameter were set to 13 and 0.0004 respectively. α and β were set to 0.84 and 0.58 respectively.

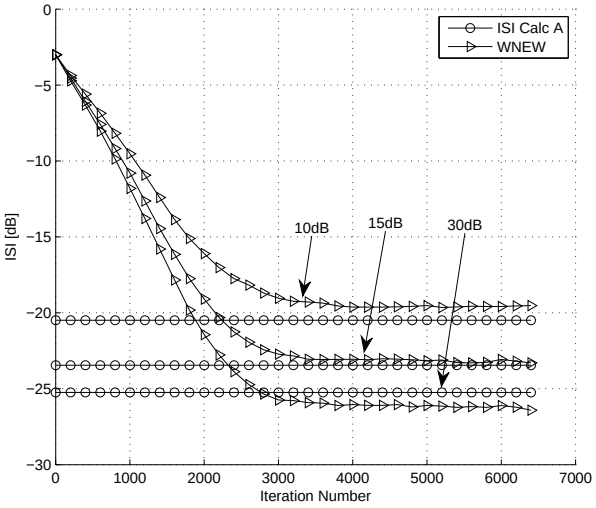

Fig. 5. A comparison between the simulated (with WNEW algorithm) and calculated residual ISI (9) (ISI Calc A) for the 16QAM source going through Channel 2 with various SNR values. The averaged results were obtained in 100 Monte Carlo trials. The equalizer's tap length and step-size parameter were set to 21 and 0.0002 respectively. α and β were set to 0.84 and 0.58 respectively.

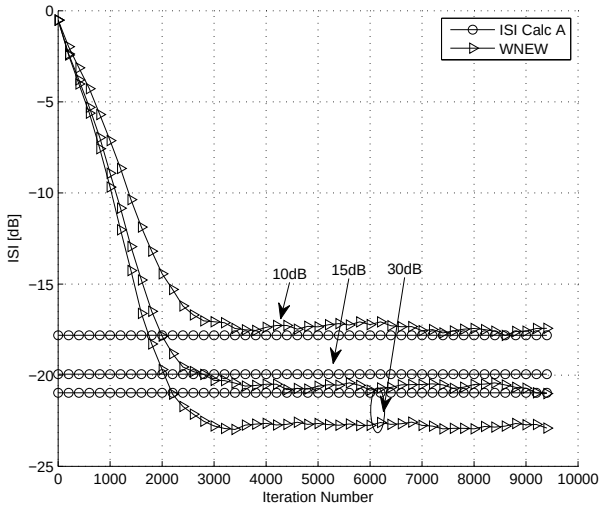

Fig. 6. A comparison between the simulated (with WNEW algorithm) and calculated residual ISI (9) (ISI Calc A) for the 64QAM source going through Channel 3 with various SNR values. The averaged results were obtained in 100 Monte Carlo trials. The equalizer's tap length and step-size parameter were set to 13 and 8e-5 respectively. α and β were set to 0.84 and 0.58 respectively.

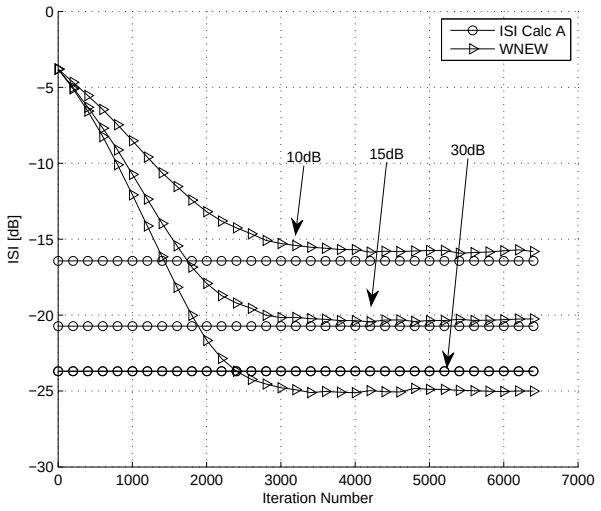

Fig. 7. A comparison between the simulated (with WNEW algorithm) and calculated residual ISI (9) (ISI Calc A) for the 16QAM source going through Channel 4 with various SNR values. The averaged results were obtained in 100 Monte Carlo trials. The equalizer's tap length and step-size parameter were set to 27 and 0.0004 respectively. α and β were set to 0.84 and 0.58 respectively.

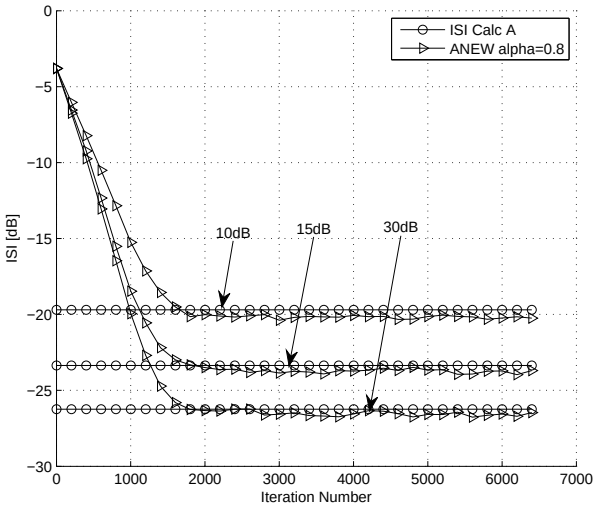

Fig. 8. A comparison between the simulated (with ANEW algorithm) and calculated residual ISI (9) (ISI Calc A) for the 16QAM source going through Channel 1 with various SNR values. The averaged results were obtained in 100 Monte Carlo trials. The equalizer's tap length and step-size parameter were set to 13 and 0.0004 respectively. α and β were set to 0.8 and 0.73 respectively.

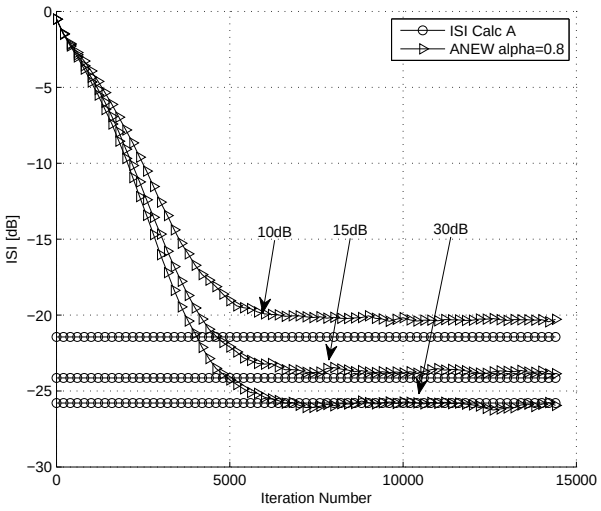

Fig. 9. A comparison between the simulated (with ANEW algorithm) and calculated residual ISI (9) (ISI Calc A) for the 64QAM source going through Channel 3 with various SNR values. The averaged results were obtained in 100 Monte Carlo trials. The equalizer's tap length and step-size parameter were set to 13 and 0.00005 respectively. α and β were set to 0.8 and 0.73 respectively.

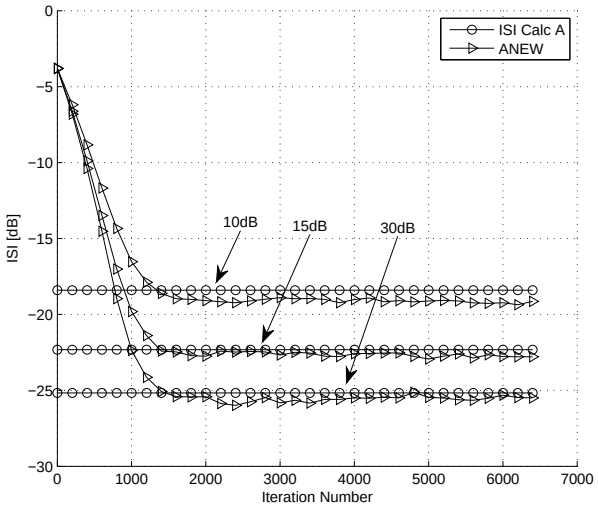

Fig. 10. A comparison between the simulated (with ANEW algorithm) and calculated residual ISI (9) (ISI Calc A) for the 16QAM source going through Channel 1 with various SNR values. The averaged results were obtained in 100 Monte Carlo trials. The equalizer's tap length and step-size parameter were set to 13 and 0.0004 respectively. α and β were set to 1 and 0.93 respectively.

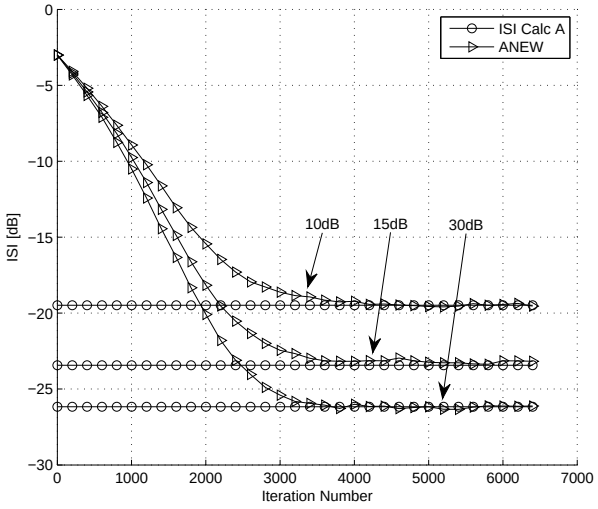

Fig. 11. A comparison between the simulated (with ANEW algorithm) and calculated residual ISI (9) (ISI Calc A) for the 16QAM source going through Channel 2 with various SNR values. The averaged results were obtained in 100 Monte Carlo trials. The equalizer's tap length and step-size parameter were set to 21 and 0.0002 respectively. α and β were set to 1 and 0.93 respectively.

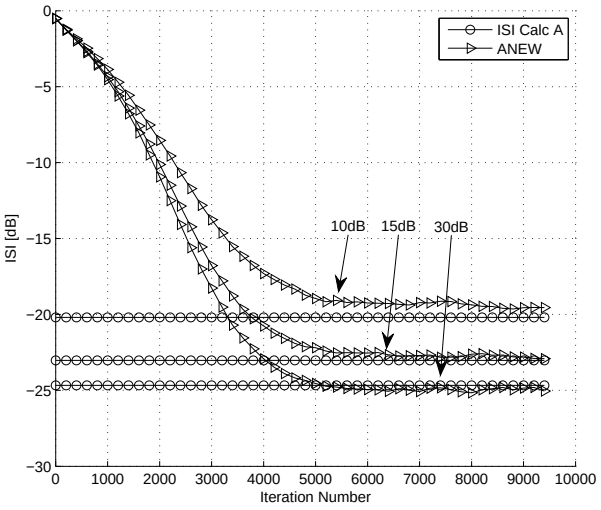

Fig. 12. A comparison between the simulated (with ANEW algorithm) and calculated residual ISI (9) (ISI Calc A) for the 64QAM source going through Channel 3 with various SNR values. The averaged results were obtained in 100 Monte Carlo trials. The equalizer's tap length and step-size parameter were set to 13 and 0.00005 respectively. α and β were set to 1 and 0.93 respectively.

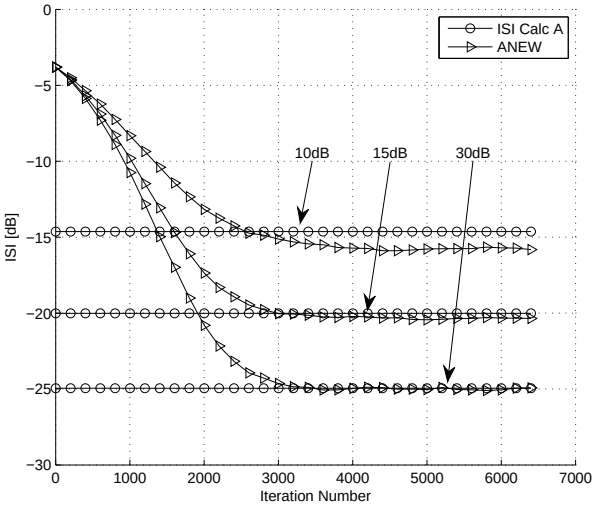

Fig. 13. A comparison between the simulated (with ANEW algorithm) and calculated residual ISI (9) (ISI Calc A) for the 16QAM source going through Channel 4 with various SNR values. The averaged results were obtained in 100 Monte Carlo trials. The equalizer's tap length and step-size parameter were set to 27 and 0.0004 respectively. α and β were set to 1 and 0.93 respectively.

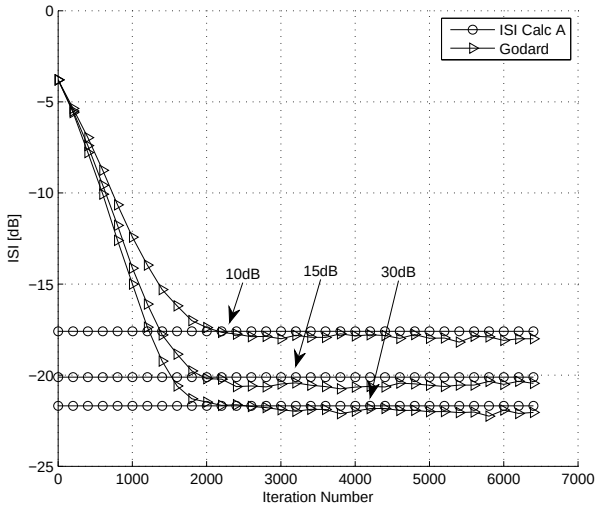

Fig. 14. A comparison between the simulated (with Godard algorithm) and calculated residual ISI (9) (ISI Calc A) for the 16QAM source going through Channel 1 with various SNR values. The averaged results were obtained in 100 Monte Carlo trials. The equalizer's tap length and step-size parameter were set to 13 and 5e-5 respectively. α and β were set both to 1.

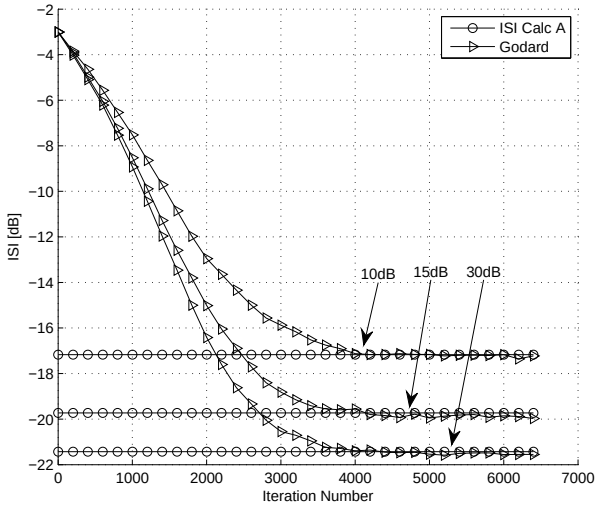

Fig. 15. A comparison between the simulated (with Godard algorithm) and calculated residual ISI (9) (ISI Calc A) for the 16QAM source going through Channel 2 with various SNR values. The averaged results were obtained in 100 Monte Carlo trials. The equalizer's tap length and step-size parameter were set to 21 and 2e-5 respectively. α and β were set both to 1.

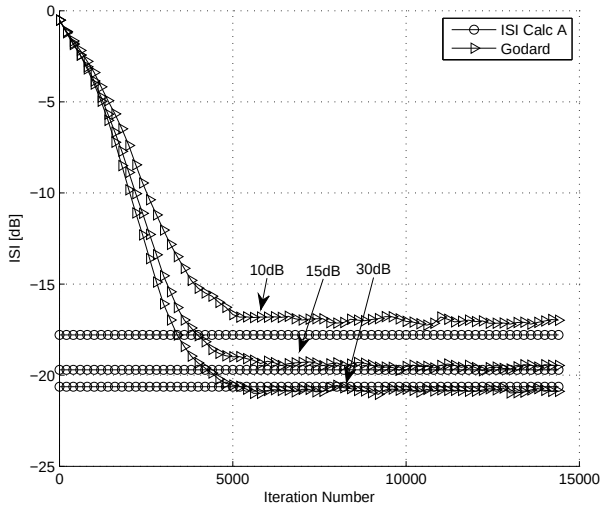

Fig. 16. A comparison between the simulated (with Godard algorithm) and calculated residual ISI (9) (ISI Calc A) for the 64QAM source going through Channel 3 with various SNR values. The averaged results were obtained in 100 Monte Carlo trials. The equalizer's tap length and step-size parameter were set to 13 and 1.2e-6 respectively. α and β were set both to 1.

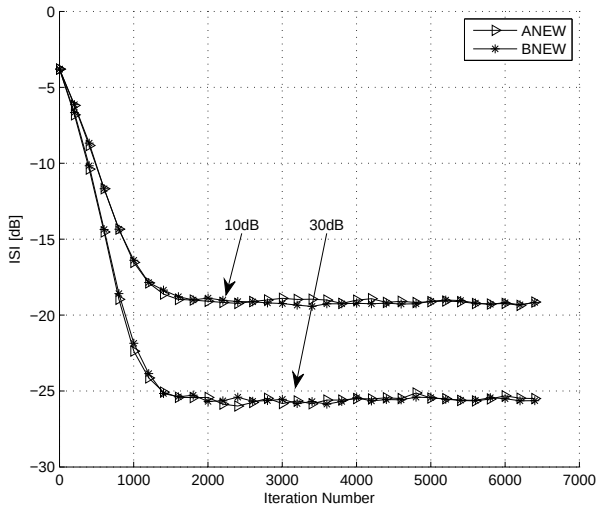

Fig. 17. A comparison between the ANEW and BNEW algorithm for the 16QAM source going through Channel 1 with SNR values of 10 dB and 30 dB. The averaged results were obtained in 100 Monte Carlo trials. The equalizer's tap length and step-size parameter were set to 13 and 0.0004 respectively. The parameter α was set to 1.

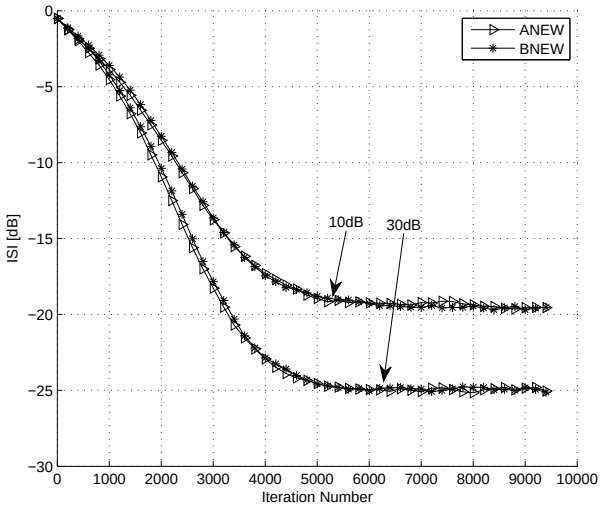

Fig. 18. A comparison between the ANEW and BNEW algorithm for the 64QAM source going through Channel 3 with SNR values of 10 dB and 30 dB. The averaged results were obtained in 100 Monte Carlo trials. The equalizer's tap length and step-size parameter were set to 13 and 0.00005 respectively. The parameter α was set to 1.

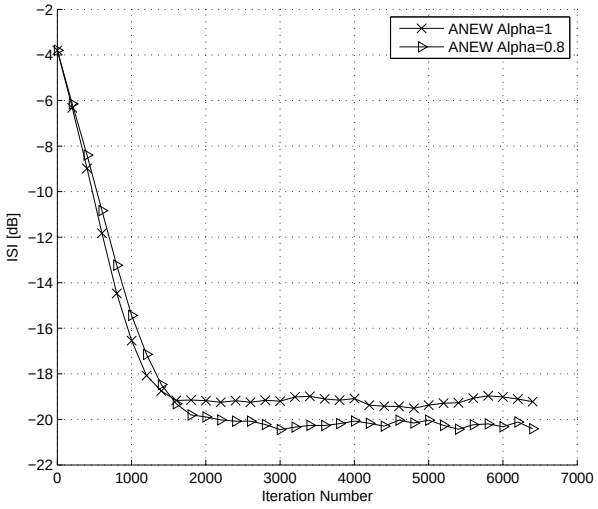

Fig. 19. A comparison between ANEW with gain $\alpha = 0.8$ and ANEW with gain $\alpha = 1$ for the 16QAM source going through Channel 1. The averaged results were obtained in 100 Monte Carlo trials. The equalizer's tap length and step-size parameter were set to 13 and 0.0004 respectively, SNR was set to 10 dB. The equalizer with gain $\alpha = 0.8$ achieves lower residual ISI by approximately 1 dB.

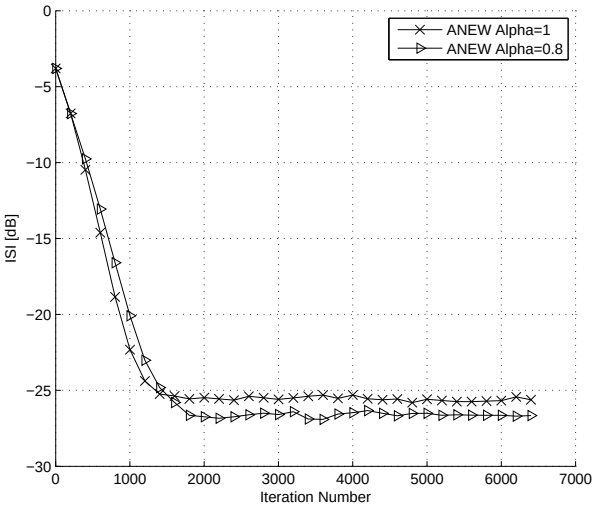

Fig. 20. A comparison between ANEW with gain $\alpha = 0.8$ and ANEW with gain $\alpha = 1$ for the 16QAM source going through Channel 1. The averaged results were obtained in 100 Monte Carlo trials. The equalizer's tap length and step-size parameter were set to 13 and 0.0004 respectively, SNR was set to 30 dB. The equalizer with gain $\alpha = 0.8$ achieves lower residual ISI by approximately 1 dB.

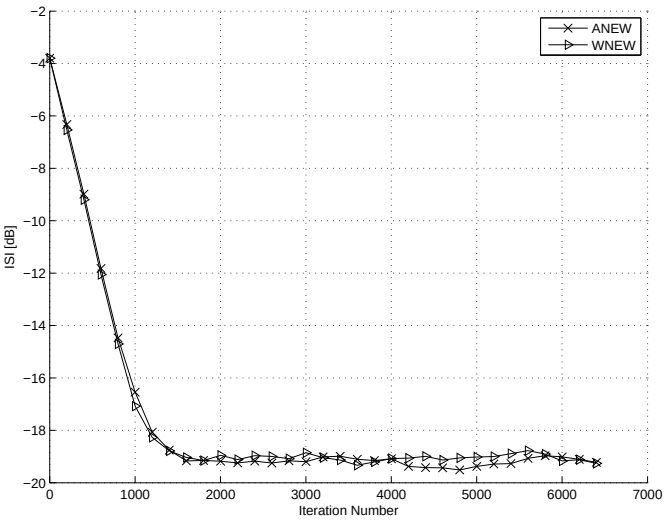

Fig. 21. A comparison between WNEW and ANEW algorithm for the 16QAM source going through Channel 1. The averaged results were obtained in 100 Monte Carlo trials. The equalizer's tap length was set to 13, the step-size parameter for WNEW and ANEW were set to $\mu_W = 0.0004$ and $\mu_A = 0.0004$ respectively, SNR was set to 10 dB. The gain α for ANEW equalizer was set to 1.

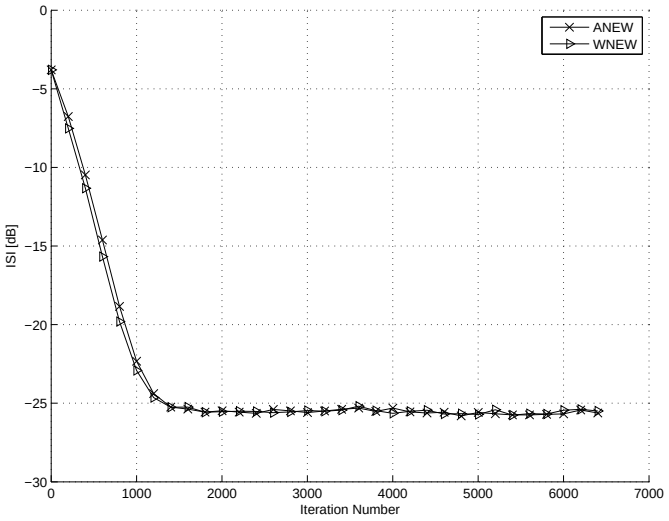

Fig. 22. A comparison between WNEW and ANEW algorithm for the 16QAM source going through Channel 1. The averaged results were obtained in 100 Monte Carlo trials. The equalizer's tap length was set to 13, the step-size parameter for WNEW and ANEW were set to $\mu_W = 0.0004$ and $\mu_A = 0.0004$ respectively, SNR was set to 30 dB. The gain α for ANEW equalizer was set to 1.

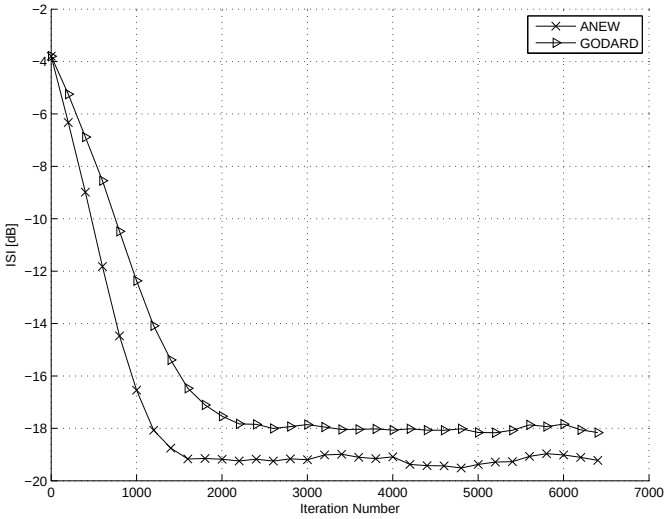

Fig. 23. A comparison between Godard and ANEW algorithm for the 16QAM source going through Channel 1. The averaged results were obtained in 100 Monte Carlo trials. The equalizer's tap length was set to 13, the step-size parameter for Godard and ANEW were set to $\mu_G = 0.00003$ and $\mu_A = 0.0004$ respectively, SNR was set to 10 dB. The gain α for ANEW equalizer was set to 1.

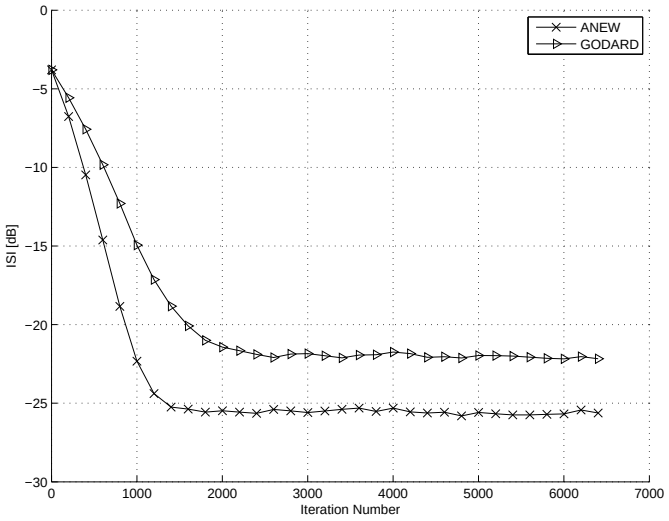

Fig. 24. A comparison between Godard and ANEW algorithm for 16QAM source input going through Channel 1. The averaged results were obtained in 100 Monte Carlo trials. The equalizer's tap length was set to 13, the step-size parameter for Godard and ANEW were set to $\mu_G = 0.00003$ and $\mu_A = 0.0004$ respectively, SNR was set to 10 dB. The gain α for ANEW equalizer was set to 1.

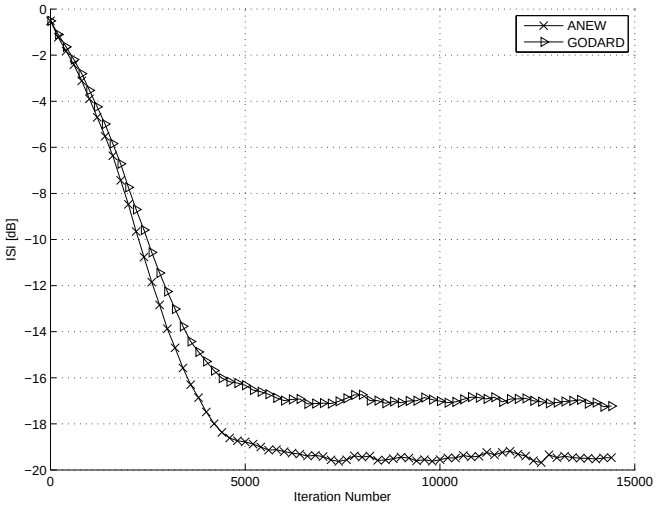

Fig. 25. A comparison between Godard and ANEW algorithms for the 64QAM source going through Channel 3. The averaged results were obtained in 100 Monte Carlo trials. The equalizer's tap length was set to 13, the step-size parameter for Godard and ANEW were set to $\mu_G = 0.0000012$ and $\mu_A = 0.00005$ respectively, SNR was set to 10 dB. The gain α for ANEW equalizer was set to 1.

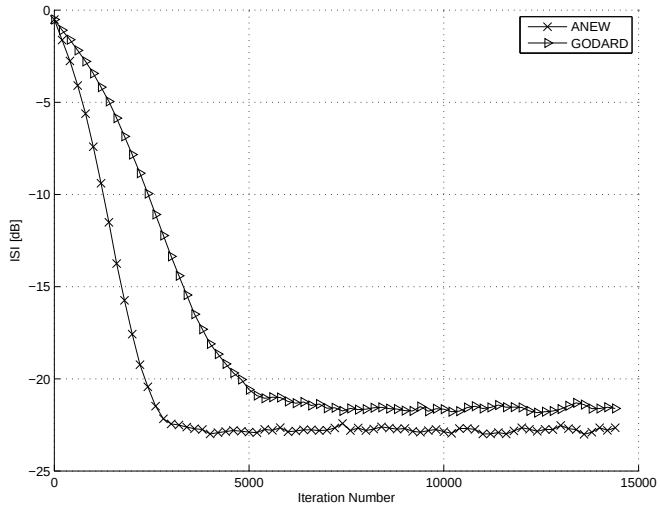

Fig. 26. A comparison between Godard and ANEW algorithm for the 64QAM source going through Channel 3. The averaged results were obtained in 100 Monte Carlo trials. The equalizer's tap length was set to 13, the step-size parameter for Godard and ANEW were set to $\mu_G = 0.000001$ and $\mu_A = 0.00008$ respectively, SNR was set to 30 dB. The gain α for ANEW equalizer was set to 1.

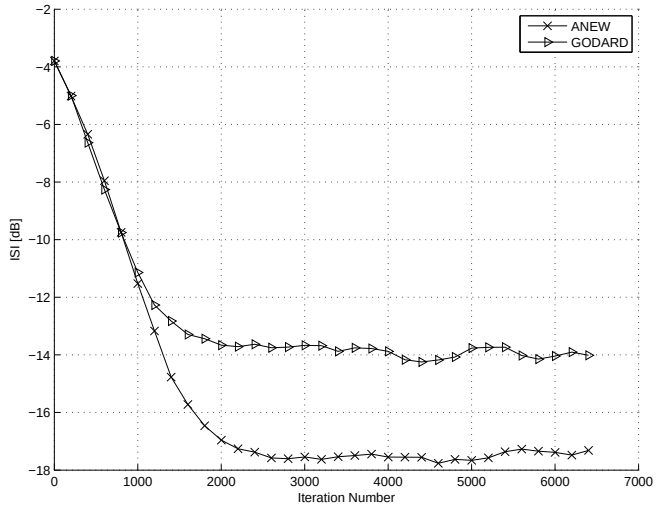

Fig. 27. A comparison between Godard and ANEW algorithms for the 16QAM source going through Channel 4. The averaged results were obtained in 100 Monte Carlo trials. The equalizer's tap length was set to 13, the step-size parameter for Godard and ANEW were set to $\mu_G = 0.00008$ and $\mu_A = 0.0006$ respectively, SNR was set to 10 dB. The gain α for ANEW equalizer was set to 1.

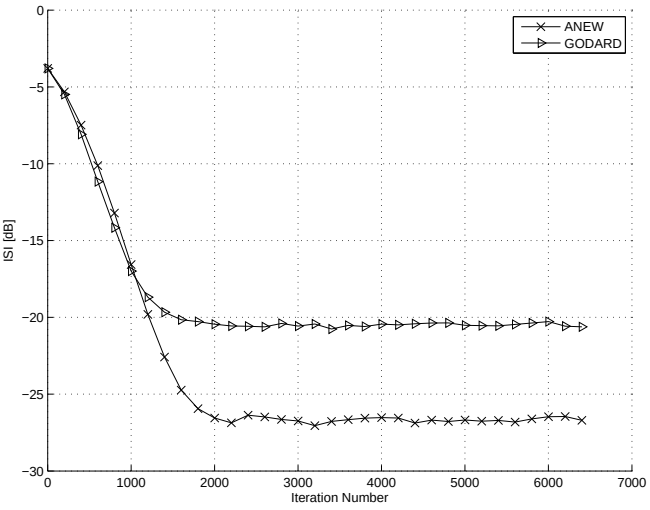

Fig. 28. A comparison between Godard and ANEW algorithms for the 16QAM source going through Channel 4. The averaged results were obtained in 100 Monte Carlo trials. The equalizer's tap length was set to 13, the step-size parameter for Godard and ANEW were set to $\mu_G = 0.00008$ and $\mu_A = 0.0006$ respectively, SNR was set to 30 dB. The gain α for ANEW equalizer was set to 1.